

Quantum entanglement and fixed-point bifurcations

Andrew P. Hines, G.J. Milburn, and Ross H. McKenzie
 Centre for Quantum Computer Technology, School of Physical Sciences,
 The University of Queensland, St Lucia, QLD 4072, Australia
 (Dated: February 9, 2020)

How do the classical dynamics of a composite system relate to the entanglement characteristics of the corresponding quantum system? We show that entanglement in nonlinear bipartite systems can be associated with a fixed point bifurcation in the classical description. In a non dissipative system a fixed point corresponds to a quantum stationary state, usually a ground state. Using the example of coupled giant spins we show that, when the fixed point undergoes a supercritical pitchfork bifurcation, the corresponding quantum state achieves a maximum amount of entanglement. By way of contrast, we consider a molecular BEC system that experiences a different kind of bifurcation and does not exhibit a peak in the entanglement corresponding to the bifurcation parameter.

I. INTRODUCTION

With the advent of quantum information theory, entanglement is now regarded as a physical resource that can be utilized to perform numerous quantum computational and communication tasks. This has in turn led to the study of the entanglement characteristics of various systems, and in turn, how these characteristics relate to better known properties of the system. Such studies have two benefits - by further elucidating the nature of entanglement as well as providing a new approach to the study of complex, quantum many-body systems.

One area where such an approach has had some success is in the study of *quantum phase transitions* (QPTs) - qualitative changes in the ground state of a multi-partite system induced by the variation of some external parameter. There have been many recent studies relating entanglement and QPTs (see [1, 2, 3, 4, 5, 6]) and that make use of the QPT to create entangled states [7].

Generally it has been found that in infinite systems that undergo a quantum phase transition at a critical parameter value $\lambda = \lambda_c$ that the entanglement as a function of λ is a maximum at $\lambda = \lambda_c$. Several examples include: (i) The single site entanglement and the next nearest neighbour concurrence of the transverse Ising chain [1, 2, 3]. (Although the nearest neighbour concurrence does not have its maximum value at $\lambda = \lambda_c$, its first derivative with respect to λ does [2]), (ii) the entropy of entanglement of half of a XXZ spin chain in a magnetic field [4], and (iii) the entropy of entanglement of a single qubit with a bath of oscillators (the spin-boson model) [5]. Such systems demonstrate a correspondence between quantum critical phenomena and entanglement.

In this article, we consider what the *classical* critical behaviour of a system can tell us about the corresponding quantum entanglement. The notion of quantum-classical correspondence dates back to Bohr and has more recently been investigated in coupled spin systems [8, 9, 10, 11]. Systems of interacting spins have been proposed as implementations of solid-state quantum computers, such as the Kane proposal [12].

The notion of relating classical properties of a system with the entanglement characteristics in the quan-

tum regime has received some attention. For example, Berman *et al.*[11] considered the detection of entangled states in macroscopic spin systems as deviations from quasi-classical dynamics. Fujisaki *et al.* recently considered the relation between classical chaos and entanglement in a system of weakly coupled, kicked tops [13].

In their work on the collective angular momentum model known as the Dicke model, Schneider and Milburn [14] found that the entanglement in the steady state of this system is a maximum for the parameter values corresponding to a bifurcation of the fixed points in the corresponding classical dynamics. Here it was conjectured that the loss of stability of a classical fixed point due to such a bifurcation will generically be associated with entanglement in the steady state of the full quantum system.

In this article we further consolidate this conjecture for non-dissipative systems by specifying the *nature* of the bifurcation which gives rise to the entanglement characteristics in the quantum system. Interestingly, we will see examples of systems whose stationary states are, somewhat counter-intuitively, not maximally entangled when the interaction between the two subsystems is maximized. The main focus of this paper can be summarized in the following conjecture:

Conjecture (Ground state entanglement)

Consider a quantum Hamiltonian $\hat{H}(g)$ which depends smoothly on a parameter g and which acts on a bipartite Hilbert space $V_1(P) \otimes V_2(P)$. The parameter P allows one to take a well-defined classical limit. Suppose that $\mathcal{H}(g)$ is the well-defined classical limit of $\hat{H}(g)$ and that there is a supercritical pitchfork bifurcation of the fixed points at the critical parameter, $g = g_c$. Let the von Neumann, entropy S , be the measure of entanglement. Then $S(g)$, the entanglement of the ground state of $\hat{H}(g)$, is a maximum with respect to g at $g_{qc}(S)$ where $g_{qc}(S) \rightarrow g_c$ in the classical limit.

We investigate the characteristics of three, two-component systems, two of which are motivated by a proposed physical implementation for quantum computation [15]. In this proposal, the qubits are realized by

magnetic clusters - nanometer scale molecular clusters that have all the attributes of mesoscopic systems such as angular momentum and magnetic moment. Two qubit gates are constructed by the coupling of the clusters (or, as we will refer to them, spinning tops) via superconducting quantum interference devices (or SQUIDS), as shown in figure 1.

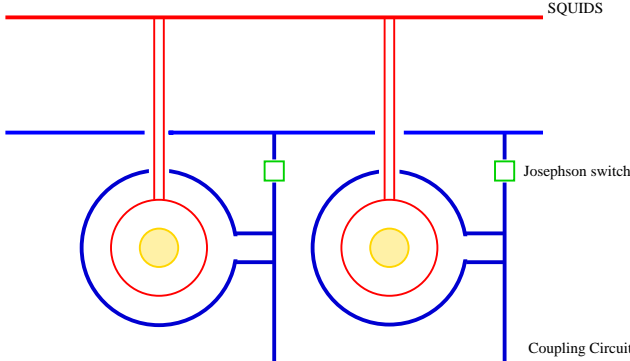


FIG. 1: A schematic diagram of the coupled qubit realization of Ref.[15]. The magnetic clusters (the qubits) are coupled to superconducting loops of micro-SQUIDS and arranged in a 1D lattice. Josephson junction switches are used in the coupling circuits, as shown.

The strength of the coupling is dependent upon the super-current induced in the loop by one spin and the field this produces at the other site [15]. This results in an interaction term of the form $\hat{H}_{int} = \hat{J}_z \otimes \hat{J}_z$. Such an interaction produces a rotation about the 'z'-axis of one cluster with frequency proportional to the z-component of the angular momentum of the other cluster - hence the nonlinear interaction. In this way, we can imagine the system as a set of spinning 'tops', coupled via a nonlinear interaction.

This article is structured as follows: In Sec. II we introduce relevant background material and a correspondence principle between fixed points and ground states. We introduce the Husimi function as the appropriate quantum analogue of a classical phase space distribution and related its structure to entanglement. Sec. III considers the ideal situation of two linear, coupled tops, whose classical dynamics have been studied extensively by Skellett and Holmes [16]. Following a derivation of the semi-classical model and an analysis of the fixed point structure and bifurcations, the entanglement in the ground state of the linear coupled spin system is investigated providing numerical evidence in support of our conjecture. Furthermore, the Husimi distributions of the ground state for various parameter values are considered.

As a contrast, in Sec. IV we consider the two-mode atom-molecule Bose-Einstein condensate, whose classical description exhibits a different type of bifurcation and whose entanglement characteristics are not related to the bifurcation. In Sec. V, the study of the coupled spin

system is extended to a more realistic case of *nonlinear* coupled tops.

II. BACKGROUND AND THEORY

This section contains the background material necessary for the analysis of the model systems used to demonstrate conjecture 1 in the remainder of the paper. We begin with a brief introduction to fixed points and bifurcations followed by a definition of the measure of entanglement we employ. Finally, we introduce a recently derived quantum-classical correspondence result [17], relating the fixed points of the classical system with the structure of the Husimi function of the ground state of the quantum Hamiltonian and discuss how the argument behind our conjecture.

A. Fixed Points and Bifurcations

An autonomous dynamical system in n -dimensional phase-space, with phase-space coordinates denoted by $\mathbf{x} = [x^{(1)} x^{(2)} \dots x^{(n)}]^T$, can be described by the set of first-order differential equations

$$\dot{\mathbf{x}} = \mathbf{F}(\mathbf{x}, g)$$

where

$$\mathbf{F}(\mathbf{x}, g) = \begin{bmatrix} f^{(1)}(\mathbf{x}, g) \\ f^{(2)}(\mathbf{x}, g) \\ \vdots \\ f^{(n)}(\mathbf{x}, g) \end{bmatrix},$$

and g is some parameter. The fixed points of the system (for a fixed g) are the coordinates where the velocity of the phase-space flow is zero, so are the roots of $\mathbf{F}(\mathbf{x}) = 0$. The stability [37] of a fixed point - putting it simply, whether nearby phase-space flows remain near or not - is determined by the analysis of the linearized matrix about that fixed point [18]. The linearized matrix about that fixed point \mathbf{x}_0 is the Jacobian matrix $\mathbf{D}f$, of $\mathbf{F}(\mathbf{x}, g)$ about \mathbf{x}_0 , whose ab^{th} element is given by

$$\mathbf{D}\mathbf{F}(\mathbf{x}_0, g)_{ab} = \frac{\partial f^{(a)}(\mathbf{x}, g)}{\partial x_b}.$$

If the eigenvalues of the linearized matrix are the set $\{\lambda_i\}$ for $i = 1, \dots, n$, the the criterion for stability about the fixed point \mathbf{x}_0 is

$$|\Re(\lambda_i)| < 1, \forall i = 1, \dots, n, \quad (1)$$

i.e. the absolute value of the real part of all eigenvalues must be less than 1 for the fixed point to be stable. Analysis of the fixed points of a dynamical system provides a qualitative description of the characteristics of the phase portrait - the trajectories in phase space.

A *bifurcation* of a fixed point(s) occurs at a critical value of some parameter of the system and results in a qualitative change in the phase portrait of the system. At the critical value, a formally stable fixed point loses its stability and, depending on the nature of the bifurcation, other fixed points may be created, destroyed or change stability. In this article, we will come across two types of bifurcation, known as *pitchfork* and *transcritical*. It is the supercritical pitchfork bifurcation that is of the most interest here. Figure 2, gives a simple, one-dimensional example of each of these two types of bifurcation.

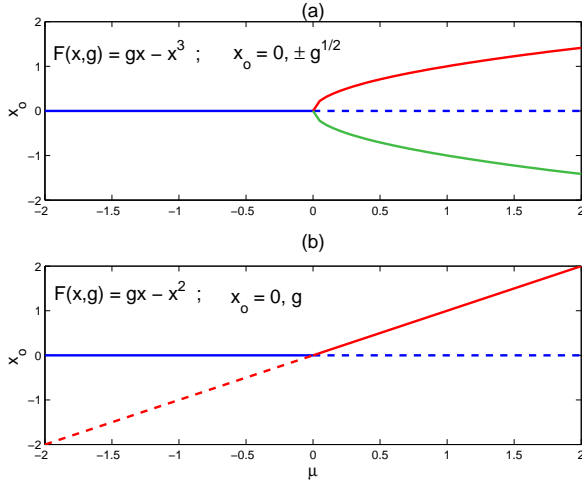


FIG. 2: Bifurcation diagrams exhibiting (a) a pitchfork bifurcation and (b) a transcritical bifurcation, with the critical parameter $g = 0$. A solid line represents a stable fixed point, while dashed represents unstable. (a) is in fact, a supercritical pitchfork, where one stable point becomes unstable and two, new stable points emerge at the bifurcation.

The basis of our conjecture lies in the comparison of classical phase space and its quantum analogue. Most importantly, how the classical fixed point structure corresponds to the structure of the analogous quantum stationary state, and in turn what this means for the entanglement. Before we continue, it is necessary to define some measure of entanglement.

B. Entanglement Measures

At present there is no definitive measure for entanglement between three or more subsystems. Such a measure is difficult to conceptualize, as there exist many distinct entanglement classes. For bipartite systems, however, pure-state entanglement is well-understood.

The canonical measure of entanglement for pure-state bipartite systems is the *entropy of entanglement* [19, 20],

$$S(\rho_i) = -\text{Tr}(\rho_i \log(\rho_i)) \quad (2)$$

where $\rho_i = \text{Tr}_i(\rho)$, is the reduced density matrix and the logarithm is taken to base 2. From the Schmidt decomposition of pure states (pg. 109 of [20]), we can choose either subsystem in the entanglement calculation without loss of generality. If $\{\lambda_i\}$ is the set of eigenvalues of the reduced density matrix ρ_1 , then the entropy of entanglement is given by

$$S(\rho_1) = -\sum_i \lambda_i \log(\lambda_i). \quad (3)$$

The entropy of entanglement takes values from 0 for a non-entangled, separable state, to a maximum value of $\log d$, where d is the dimension of the subsystems. For qubits, the maximum entanglement is 1, and corresponds to the (maximally entangled) Bell states, $(|00\rangle \pm |11\rangle)$ and $(|01\rangle \pm |10\rangle)$. For qudits (the d -dimensional analogue of the qubit), a maximally entangled state takes the form

$$\frac{1}{\sqrt{d}} \sum_{k=0}^{d-1} |k, k\rangle \quad (4)$$

or,

$$\frac{1}{\sqrt{d}} \sum_{i=0}^{d-1} |k, d-1-k\rangle = \frac{1}{\sqrt{d}} |0, d-1\rangle + |1, d-2\rangle + \dots + |d-1, 0\rangle. \quad (5)$$

In contrast the qudit analogue of the Bell (or EPR) states,

$$|EPR\rangle = \frac{1}{\sqrt{2}} (|kl\rangle \pm |lk\rangle) \quad (6)$$

$(0 \leq k \neq l \leq d-1)$ have entanglement of 1 regardless of the dimension of the system.

With these different entangled states in mind, we now consider how the classical fixed points govern the structure of the quantum stationary states, and how this leads to somewhat non-intuitive entanglement characteristics of the ground state.

C. Quantum-classical correspondence

Fundamental to any comparison of classical and quantum dynamics is some notion of the quantum analogue of a classical joint phase-space probability distribution. Classical dynamics are conveniently studied in a phase-space representation [21]. On the other hand, the inherent probabilistic nature of quantum mechanics means that we cannot discuss points in phase-space when referring to quantum states. Furthermore, the Heisenberg uncertainty principle makes it difficult to describe a true joint phase-space probability density in quantum mechanics [22]. Such an object, however would make the comparison of classical and quantum dynamics straightforward, by simple comparison of the dynamics of the relevant densities.

One path to an appropriate phase space description is to construct, from the quantum states, a joint probability density function for simultaneous measurements of position and momentum. Such a view leads to the Husimi or Q -function as the appropriate quantum analogue of the classical phase-space density. While there have been many attempts to define a quantum joint probability distribution (such as the Wigner function [23]), many (see Refs.[8, 21, 22, 24, 25, 26]) consider the Q -function as the appropriate quantum analogue of the classical phase-space density.

The Q -function is a true probability density, defined as the matrix elements of the quantum density operator in the coherent state basis [8]. For topologically flat phase space, such as for the harmonic oscillator in quantum optics, these are the coherent states of the Heisenberg-Weyl group, and the resulting Q -function is the distribution for simultaneous measurements of position and momentum [8].

For systems described in spherical phase-space, Appleby [27] demonstrated that the positive operator valued measurement (POVM) for optimal simultaneous measurements of components of angular momentum is given by

$$\hat{E}(z) = |z\rangle\langle z| \quad (7)$$

where $|z\rangle$ are the $SU(2)$ coherent states [28], defined by

$$\begin{aligned} |z\rangle &= (1 + |z|^2)^{-j} e^{z\hat{J}_+} |j, -j\rangle \\ &= (1 + |z|^2)^{-j} \sum_{n=0}^{2j} \binom{2j}{n}^{1/2} z^n |j, -j + n\rangle \end{aligned} \quad (8)$$

where $|j, m\rangle$ are again the eigenstates of \hat{J}_z with eigenvalue m and z is the stereographic projection of the sphere

$$z(\theta, \phi) = e^{-i\phi} \tan \frac{\theta}{2}. \quad (9)$$

The angular momentum representation Q -function, which is interpreted as the probability distribution for measurements defined by the POVM, for pure state $|\psi\rangle$ is thus

$$Q_\psi(z) = \text{Tr}(\rho \hat{E}(z)) = |\langle z|\psi\rangle|^2. \quad (10)$$

The Q -function representation is extended to many-body-systems by defining the appropriate coherent states. This can be done in several ways. So as to retain the view of the many-body system in terms of distinct subsystems, following Sugita [29], we use the Gilmore-Perelomov coherent states of the single-particle (or local unitary) transformation group [28, 30] (throughout the paper, the term ‘coherent state’ will refer to these specific states). The coherent states are generated by applying this group to the lowest (or highest) weight state. Importantly, this means that all separable (hence disentangled) states are generated in this way, such that a

coherent state (by our definition) is equivalent to a separable state.

In terms of a system of m subsystems each with spin J , the single-particle transformation group is $SU(2J+1)^{\otimes m}$, and the coherent states are

$$|z\rangle = |z_1\rangle \otimes \dots \otimes |z_m\rangle \quad (11)$$

and the corresponding Q -function is defined as in Eq. 10.

In the case of our composite, coupled tops systems, we have two subsystems making the Q -function

$$Q_\psi(z_1, z_2) = |\langle (z_1 \otimes z_2) |\psi\rangle|^2. \quad (12)$$

The Q -function has been used extensively in work on classical-quantum correspondence, in particular, in studies of quantum chaos (for examples see Refs. [25, 26]). In such driven dynamical studies, it has been demonstrated that Q -function distributions localized in regular (non-chaotic) regions of classical phase space will remain localized over the evolution. Conversely, distributions initially localized in chaotic regions become delocalized throughout the chaotic region. Such behavior highlights the correspondence with analogues classical phase-space distributions.

But how do fixed points and bifurcations manifest in the quantum regime? The answer to this question is contained in the following result;

Fixed point correspondence principle: *Let \hat{H} be a Hamiltonian whose classical analogue is defined as $\mathcal{H}(\chi, \chi^*) = \langle \chi | \hat{H} | \chi \rangle$, where $\{|\chi\rangle\}$, is the set of coherent states corresponding to the topology of the phase-space of $\mathcal{H}(\chi, \chi^*)$. Then the Husimi distribution of the ground state of \hat{H} will attain maximum value(s) on the phase-space coordinates corresponding to the fixed point(s) of \mathcal{H} .*

A detailed proof of this result is given in Ref. [17].

Following the argument of Sugita [29], the entanglement in the state of a composite system can be related to the structure of the corresponding Q -function.

Sugita [29] argues that in many-body quantum systems delocalization of the Husimi distribution is a sign of entanglement. The term *delocalization* is used with respect to the effective phase-space volume occupied by the Q -function - the greater the effective volume, the more delocalized the distribution.

As stated before, the set of coherent states chosen to construct the Q -function of a given state is equivalent to the set of separable states. A coherent stat, and thus a separable state, by the definition of the Q -function (10) is represented by a localized (minimum effective volume) Husimi distribution. Hence delocalization of the Q -function distribution corresponds to entanglement.

This notion is analyzed more rigorously in Ref. [29], where a measure of this delocalization, and hence the entanglement, in terms of the moment of the Q -function is proposed.

We are now in a positng to combine all of these ideas together, to link the pitchfork bifurcation in the classical

with the entangle of the ground state in the quantum regime

Imagine we have complete, adiabatic, control over the bifurcation parameter (a coupling or some other parameter) and we start with our system at the stable bifurcating fixed point where $g < g_c$. Now we begin to increase this parameter. Classically, as g approaches the bifurcation point, it will remain at the original fixed point and as it passes g_c it will ‘choose’ (with equal probability) one of the emerging stable fixed points to move onto, as the original point becomes unstable. Quantum mechanically, this is not the case.

If the quantum system is initially in an eigenstate of the Hamiltonian, the adiabatic theorem means that the systems will remain in an eigenstate as the parameter is increased adiabatically. So, below the critical value, g_c , this corresponds to a single energy eigenstate localized around the sole fixed point. Above g_c , this state connects smoothly to a new eigenstate that is a symmetric combination of states localized on the two new fixed points. Near, but on the upper side of the bifurcation, the distribution will be spread across the three fixed points, and is much more delocalized when the two emergent fixed points are close. It is this characteristic that results in a peak in the ground state entanglement corresponding to the bifurcation.

We now digress to the classical and quantum analysis of the three model systems we will use to illustrate our conjecture, beginning with the coupled linear tops.

III. COUPLED LINEAR TOPS

The quantum analogue of the classical coupled tops system investigated by Skellett and Holmes [16] can be viewed as a generalization of the $N = 2$ case of the transverse field quantum Ising model. This system is described by the Hamiltonian

$$\hat{H} = \omega \hat{J}_x \otimes \hat{I} + \omega \hat{I} \otimes \hat{J}_x + \chi \hat{J}_z \otimes \hat{J}_z \quad (13)$$

where the angular momentum operators \hat{J}_i satisfy the commutation relations $[\hat{J}_x, \hat{J}_y] = i\hat{J}_z$ (and cyclic permutations). The magnitude of the total angular momentum of the system, J , is a constant of the motion, the square of which is

$$\hat{J}^2 = \hat{J}_1^2 + \hat{J}_2^2 + 2\hat{\mathbf{J}}_1 \cdot \hat{\mathbf{J}}_2 \quad (14)$$

where J_1 and J_2 are the total angular momentums of the individual subsystems. In fact, it is easy to show that J_1 and J_2 are also constants of the motion i.e.

$$[\hat{J}^2, \hat{H}] = [\hat{J}_1^2, \hat{H}] = [\hat{J}_2^2, \hat{H}] = 0. \quad (15)$$

Furthermore, there is another constant of the motion, corresponding to the symmetry of the system to π -rotations about the \hat{J}_{xi} axes. Defining the parity operator, $\hat{\Pi}$, as

$$\hat{\Pi} = e^{i\pi(\hat{J}_{x1} + \hat{J}_{x2})} \quad (16)$$

it satisfies $[\hat{\Pi}, \hat{H}] = 0$.

Here we let $\mu = \frac{\chi}{\omega}$, resulting in a one-parameter Hamiltonian which is rewritten in the form

$$\hat{H} = \hat{J}_{x1} + \hat{J}_{x2} + \mu \hat{J}_{z1} \hat{J}_{z2} \quad (17)$$

where we make use of the notation $\hat{J}_{a1} = \hat{J}_a \otimes \hat{I}$ and $\hat{J}_{a2} = \hat{I} \otimes \hat{J}_a$, $a = x, y, z$, such that the subscript 1 (2) refers to subsystem 1 (2).

The dimension of the Hilbert space of this composite system is given by $d_1 \times d_2$, where d_i is the dimension of the Hilbert space of the i^{th} subsystem. Since we are considering two identical subsystems, $d_1 = d_2 = 2j+1$ where $\sqrt{j(j+1)}$ is the eigenvalue of the total angular momentum operator of the individual subsystems. Thus, for $j = \frac{1}{2}$, the Hamiltonian (13) is analogous to the quantum Ising model for $N = 2$ spins (see Ref. [31]),

$$\hat{H} = 2K\hat{\sigma}_z \otimes \hat{\sigma}_z + B(\hat{\sigma}_x \otimes \hat{I} + \hat{I} \otimes \hat{\sigma}_x). \quad (18)$$

Equation (18) is related to (13) by $B = \omega$ and $2K = \chi$. This Hamiltonian describes the case where the external magnetic field is perpendicular to the z axis (in the x -direction).

The analysis of the corresponding classical system [16] has shown that the non-linearity of the interaction term leads to chaotic motion for certain parameter ranges and initial conditions. One of the major results of this analysis was to show the existence of a supercritical pitchfork bifurcation of the fixed points, at a critical value of the coupling parameter. From Ref.[16] this critical value, μ_c , is given by

$$\mu_c = \frac{1}{L} \quad (19)$$

where L is the classical total angular momentum of the individual tops. Below this critical value the dynamics of the system is regular while above the phase space is mixed, with extensive regions of chaotic motion.

A. Semi-Classical Dynamics

To derive the semi-classical dynamics we begin with the Heisenberg equations of motion to find the time evolution of the angular momentum component operators for each subsystem. Using the commutation relations $[\hat{J}_{x\alpha}, \hat{J}_{y\beta}] = i\delta_{\alpha\beta}\hat{J}_z$ (and cyclic permutations, with $\alpha, \beta = 1$ or 2) we obtain the six operator equations of

motion

$$\frac{d\hat{J}_{x1}}{dt} = -\mu\hat{J}_{y1}\hat{J}_{z2} \quad (20a)$$

$$\frac{d\hat{J}_{y1}}{dt} = \mu\hat{J}_{x1}\hat{J}_{z2} - \hat{J}_{z1} \quad (20b)$$

$$\frac{d\hat{J}_{z1}}{dt} = \hat{J}_{y1} \quad (20c)$$

$$\frac{d\hat{J}_{x2}}{dt} = -\mu\hat{J}_{z1}\hat{J}_{y2} \quad (20d)$$

$$\frac{d\hat{J}_{y2}}{dt} = \mu\hat{J}_{z1}\hat{J}_{x2} - \hat{J}_{z2} \quad (20e)$$

$$\frac{d\hat{J}_{z2}}{dt} = \hat{J}_{y2} \quad (20f)$$

To take the semi-classical limit of the above differential equations, we first consider the correlation function between two operators, \hat{X}, \hat{Y} ,

$$\langle \hat{X}, \hat{Y} \rangle = \langle \hat{X} \hat{Y} \rangle - \langle \hat{X} \rangle \langle \hat{Y} \rangle, \quad (21)$$

also known as the *covariance*. In our case, all operators are elements of the $SU(2)$ group of total angular momentum operators. As such, from the scaling of the individual variances of the operators, it is relatively simple to show that, for $j(j+1)$, the eigenvalue of the square of the total angular momentum operator of each subsystem,

$$\langle \hat{X}, \hat{Y} \rangle = \mathcal{O}(\sqrt{j(j+1)}). \quad (22)$$

i.e., the covariance is of order not exceeding j . Conversely, both $\langle \hat{X} \hat{Y} \rangle$ and $\langle \hat{X} \rangle \langle \hat{Y} \rangle$ are (clearly) $\mathcal{O}(j(j+1))$. Re-expressing Eq. (21), and dividing through by $j(j+1)$ yields

$$\frac{\langle \hat{X} \hat{Y} \rangle}{j(j+1)} = \frac{\langle \hat{X} \rangle}{\sqrt{j(j+1)}} \frac{\langle \hat{Y} \rangle}{\sqrt{j(j+1)}} + \mathcal{O}\left(\frac{1}{\sqrt{j(j+1)}}\right) \quad (23)$$

which implies that in the semi-classical limit of large j

$$\frac{\langle \hat{X} \hat{Y} \rangle}{j(j+1)} \approx \frac{\langle \hat{X} \rangle}{\sqrt{j(j+1)}} \frac{\langle \hat{Y} \rangle}{\sqrt{j(j+1)}} \quad (24)$$

i.e., the expectation values of products of operators can be factorized. This leads to the definition of the semi-classical variables as,

$$L_{a\alpha} = \frac{\langle \hat{J}_{a\alpha} \rangle}{\sqrt{j(j+1)}} \quad (25)$$

which are just real numbers. Throughout the article we will use the convention that roman subscripts can take values of x, y or z , referring to the component of the angular momentum, while Greek subscripts are either 1 or 2, referring to the subsystems.

Replacing the operators in the above differential equation with these expressions results in the semi-classical

equations of motion [16]. With this definition, from the conservation of the individual subsystems total angular momentum, the motion of the tops is constrained to the spheres,

$$L_{x\alpha}^2 + L_{y\alpha}^2 + L_{z\alpha}^2 = 1 \quad (26)$$

and the critical parameter is $\mu_c = 1$.

The fixed points of the system are found by setting the equations of motion to zero, and solving for the six unknowns, making use of the constraint (26). There are four solutions which exist for all values of the parameter μ , given by

$$L_{x1} = \pm 1, L_{x2} = \pm 1, L_{z1} = L_{y1} = L_{z2} = L_{y2} = 0. \quad (27)$$

At the critical value, $\mu_c = 1$ the two fixed points at $L_{x1} = L_{x2} = 1$ and $L_{x1} = L_{x2} = -1$ under go a bifurcation, resulting in a further *four* fixed points, located at

$$L_{x1} = L_{x2} = \frac{1}{\mu}, \quad L_{z1} = L_{z2} = \pm \sqrt{1 - \frac{1}{\mu^2}}, \quad (28)$$

$$L_{y1} = L_{y2} = 0, \quad (29)$$

$$L_{x1} = L_{x2} = -\frac{1}{\mu}, \quad L_{z1} = -L_{z2} = \pm \sqrt{1 - \frac{1}{\mu^2}}, \quad (30)$$

$$L_{y1} = L_{y2} = 0 \quad (31)$$

which exist for all $\mu > 1$.

The stability of the fixed points is determined by analysis of the eigenvalues of the linearized matrix about each fixed point [18]. In Ref. [16], it was shown that the two fixed points of (27) with $L_{x1} = -L_{x2}$ are *unstable* fixed points, for all values of the parameter μ . The points, $L_{x1} = L_{x2} = \pm 1$ are stable for $\mu < 1$, then become unstable at μ . The fixed points that emerge at the critical parameter value are stable fixed points. This implies that the bifurcations occurring at $L_{x1} = L_{x2} = \pm 1$ for $\mu = 1$ are indeed supercritical pitchfork bifurcations, as illustrated in figure 2(a).

Since the total angular momenta of the two tops are conserved, their dynamics are constrained to the surface of the unit sphere in the three dimensional angular momentum space. Thus, it is possible to reformulate the dynamics in terms of spherical polar coordinates, the polar angle from the positive $L_{z\alpha}$ axis, $0 \leq \theta_\alpha \leq \pi$, and the azimuthal angle in the $L_{x\alpha} - L_{y\alpha}$ plane (from the positive $L_{x\alpha}$ axis), $0 \leq \phi_\alpha \leq 2\pi$. These coordinates give the angular momentum components via

$$\begin{aligned} L_{x\alpha} &= \sin \theta_\alpha \cos \phi_\alpha \\ L_{y\alpha} &= \sin \theta_\alpha \sin \phi_\alpha \\ L_{z\alpha} &= \cos \theta_\alpha. \end{aligned} \quad (32)$$

For all fixed points, $L_{y1} = L_{y2} = 0$, which in spherical polar coordinates, corresponds to $\phi_1, \phi_2 = 0$ or π . Thus,

we can view the fixed points as lying on the unit circle in the $L_{x\alpha} - L_{z\alpha}$ planes, characterized by the polar angles, θ_i . For μ below the critical coupling there are two, stable fixed points, both of which lie at the ‘equator’ of these unit circles ($\theta_i = \frac{\pi}{2}$) at $L_{x1} = L_{x2} = 1$ ($\phi_1 = \phi_2 = 0$) and at $L_{x1} = L_{x2} = -1$ ($\phi_1 = \phi_2 = \pi$). Following the notation used by Skellatt and Holmes [16], we denote the two states by $(\rightarrow\rightarrow)$ and $(\leftarrow\leftarrow)$ respectively, corresponding to the direction of the angular momentum vector.

For μ greater than the critical value, there are four stable fixed points, whose positions are shown in figure 3. The points labeled A and B correspond to Eq. (28)

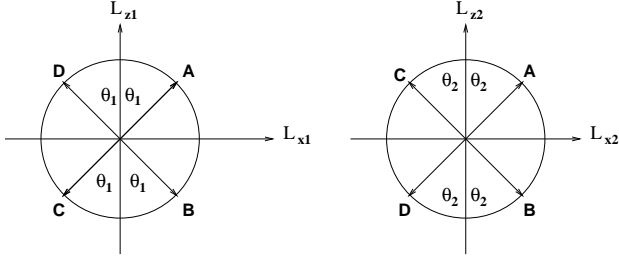


FIG. 3: The four stable fixed points for $\mu > 1$. As $\mu \rightarrow \infty$, $\theta_1, \theta_2 \rightarrow 0$, resulting in fixed points with angular momentum solely in the L_z directions, denoted $(\uparrow\uparrow)$, $(\uparrow\downarrow)$, $(\downarrow\uparrow)$ and $(\downarrow\downarrow)$.

and points C and D to Eq. (30). Clearly as $\mu \rightarrow \infty$, $\theta_i \rightarrow 0$ (in figure 3) and, in the pictorial (arrow) notation of above, we have the four fixed points at the ‘poles’ of the spheres, in the four combinations $(\uparrow\uparrow)$, $(\uparrow\downarrow)$, $(\downarrow\uparrow)$ and $(\downarrow\downarrow)$, all of which are stable.

The semi-classical analysis we have presented here is just a brief summary of those aspects most relevant for this paper. For an in-depth analysis of the classical dynamics of this system we again refer the reader to Skellatt and Holmes [16].

We now move to the quantum analysis of this system. Here we are concerned with the variation in the entanglement in the ground state with respect to μ .

B. The Quantum Regime

Both stable fixed points below the critical μ_c bifurcate and one of them will be associate with the ground state. By considering the moments, it simple to see that the ground state corresponds to the classical fixed point $L_{x1} = L_{x2} = -1$. Similarly, the highest energy state corresponds to the classical fixed point $L_{x1} = L_{x2} = 1$ which also undergoes the same type of bifurcation. Both of these states will exhibit the same entanglement characteristics with respect to the coupling parameter (see Appendix A). We restrict ourselves to the ground state.

To calculate the entropy of entanglement of the ground state we represent the Hamiltonian (17) in the basis of the tensor product of the irreducible representation of $SU(2)$ - the states $|j, m\rangle \otimes |j, n\rangle$, where $-j \leq m, n \leq j$.

We will abbreviate the basis states $|j, m\rangle \otimes |j, n\rangle$ by simply $|m, n\rangle$. The Hamiltonian is diagonalised and the ground eigenstate used to construct a density matrix, after which equation (2) can be applied.

To begin we consider the special case of two coupled spin- $\frac{1}{2}$ tops, previously studied by Gunlycke *et al.* [31].

1. Spin-Squeezing and the Spin- $\frac{1}{2}$ Case

For the two-site transverse field Ising model, equation (18), an explicit expression for the entanglement in the ground state has been derived by Gunlycke *et al.* [31]. The measure of entanglement they considered was the *tangle*, which is the square of the concurrence. The concurrence is a closed expression for the entanglement of formation E_F of two-qubit states (see Ref.[32]).

In terms of the parameters of the Hamiltonian (18) the expression for the tangle is [38]

$$\tau = \frac{K^2}{K^2 + 4B^2} = \frac{1}{1 + \mu^2}, \quad (33)$$

since $\mu = 2K/B$. The entropy of entanglement is given by the tangle via the expressions

$$S(\rho) = \mathbb{H} \left(\frac{1 + \sqrt{1 - \tau}}{2} \right). \quad (34)$$

where \mathbb{H} is the Shannon entropy function

$$\mathbb{H}(p) = -p \log_2(p) - (1 - p) \log_2(1 - p). \quad (35)$$

The evaluation of this function for the entropy of entanglement is shown in figure 4.

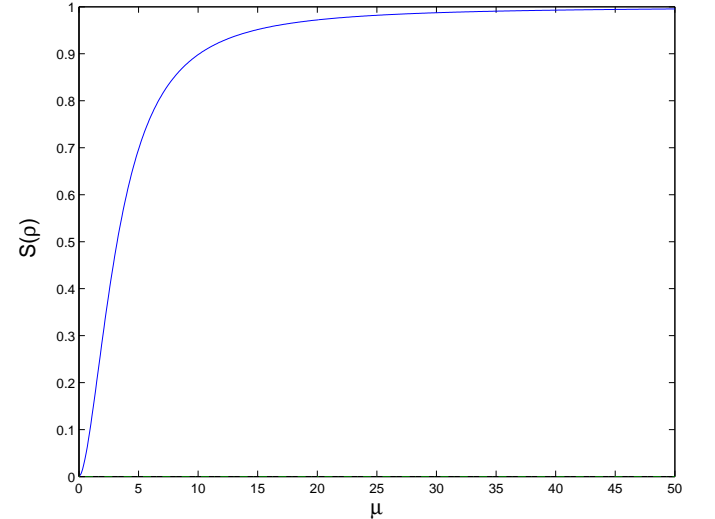


FIG. 4: Entropy of entanglement for the quantum Ising model with $N = 2$

From figure 4 we see that for the case of $j = \frac{1}{2}$, the ground state entanglement is zero for zero coupling. As

the coupling is increased, the entanglement increases, asymptotically approaching 1 - the maximum entanglement for a two-qubit system.

While this is clearly in disagreement with our conjecture, it can be explained via the Heisenberg uncertainty principle.

Central to our conjecture is the notion that in the limit of large coupling the Q -function distribution of the ground state becomes two, separated peaks localized around the fixed points corresponding to the symmetric superposition of the two bipartite coherent states making up the *EPR* state, Eq.6. Coherent state are minimum uncertainty states, satisfying equality in the Heisenberg uncertainty principle (HUP). Subsequently, a coherent state Q -function is a Gaussian distribution, with variances corresponding to the standard quantum limit (SQL), as defined by the HUP.

In the spin- $\frac{1}{2}$ case, the separation of the fixed point coordinates is the SQL, so the two coherent state distributions will overlap. At no point will the Q -function have a twin-peaked structure. The maximum entanglement still corresponds to the most delocalized Q -function, however this occurs in the limit of infinite coupling, as opposed to some finite value.

This point is illustrated in figure 5. The ground state Q -function distributions for increasing coupling strengths are shown. Graphically, we can only consider three-dimensional cross-sections of the five-dimensional Q -function. Since the fixed point(s) corresponding to the quantum ground state occur at $\phi_1 = \phi_2 = \pi$ (i.e. in the $-L_x$ half of the $L_x - L_z$ planes), we consider the cross-sections of the Q -functions on the surface $\phi_1 = \phi_2 = \pi$.

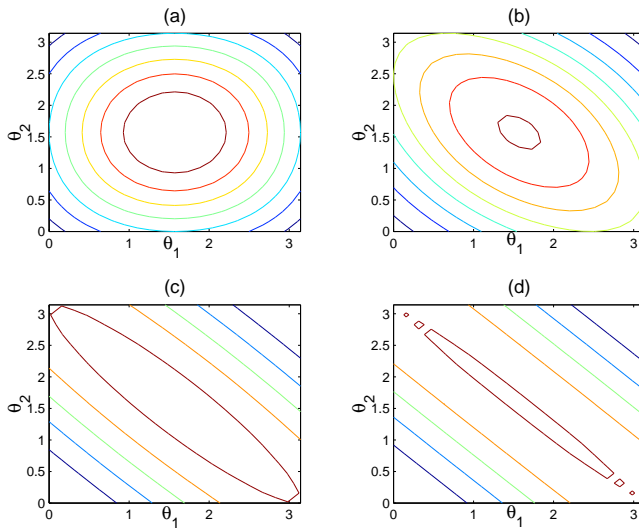


FIG. 5: The $\phi_1 = \phi_2 = \pi$ cross-section of the Q -function distribution for two coupled spin- $\frac{1}{2}$ tops (qubits), for (a) $\mu = 0$, (b) $\mu = 5$, (c) $\mu = 50$ and (d) $\mu = 500$.

Our conjecture is based on a quantum-classical correspondence principle. Put simply, the case of two inter-

acting spin- $\frac{1}{2}$ particles is *too quantum* to concur with the principle.

As a further note on the spin- $\frac{1}{2}$ case, we refer to Gunlycke *et al.* [31]. There it is argued that there exists a *quantum phase transition* at $B = 0$ (in relation to Hamiltonian (18)) where the entanglement jumps discontinuously from zero to maximal entanglement, for even infinitesimally small increases in B . It is not entirely clear that this statement is correct, as quantum phase transitions are argued to only occur in the limit of infinite dimensional systems. Here we have a finite dimensional system. A less controversial statement is to say that there is a *level crossing* of the energy eigenvalues at this point. This is characteristic of quantum phase transitions in infinite dimensional systems [33].

This apparent discontinuity in the entanglement comes from considering $B = 0$, where the Hamiltonian consists of only the interaction term, $\sigma_z \otimes \sigma_z$. It is easy to see two degenerate ground states for the interaction term are

$$|\frac{1}{2}, -\frac{1}{2}\rangle, \text{ and, } |-\frac{1}{2}, \frac{1}{2}\rangle. \quad (36)$$

This degeneracy in the ground state arises from the rotation symmetry for π -rotations about the J_x -axes, corresponding to the parity operator $\hat{\Pi}$. Both of these states are completely separable and thus disentangled, implying that there is a discontinuous jump in the entanglement. However, there are other states that are degenerate with (36), such as

$$\frac{1}{\sqrt{2}} (|\frac{1}{2}, -\frac{1}{2}\rangle \pm |-\frac{1}{2}, \frac{1}{2}\rangle). \quad (37)$$

Both of these states are maximally entangled (Bell) states, and imply there is no discontinuity in the entanglement at $B = 0$. In fact, any (normalized) linear combination of the two states (36) will be a degenerate ground state. The states (37) are the maximally entangled ground states. In other words, there are an infinite number of ground states, which will have entanglement ranging from 0 to 1 - for the spin- $\frac{1}{2}$ case, this is the full range of possible entanglement values. This degeneracy at $B = 0$ makes the calculation of the entanglement in the ground state in this limit not as clear cut as first thought. In fact, this degeneracy occurs for all values of j at infinite μ , with the states $| -j, j \rangle$ and $| j, -j \rangle$, again resulting in the entanglement being anywhere between 0 and 1. Of course, for higher dimensional systems, the maximum possible entanglement is no longer 1.

2. Entanglement and the Classical Bifurcation

For $j > \frac{1}{2}$, the entanglement characteristics of the ground state with respect to the interaction strength (μ) take on a different structure as shown in figure 6.

Here we see that for larger j , the entanglement in the ground state does not asymptote to its maximal value as $\mu \rightarrow \infty$ but rather the entanglement peaks at a finite

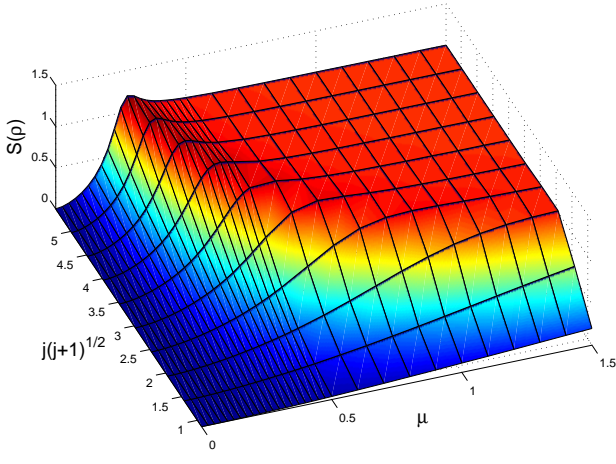


FIG. 6: Variation in the entropy of entanglement of the ground state for with respect to the coupling strength μ and the total subsystem angular momentum, $\sqrt{j(j+1)}$. Note that as the system becomes more classical as j increases that the peak in the entanglement versus μ becomes more evident.

value of μ . As well, the greater the value of j , the greater and more pronounced this maximum becomes.

To illustrate that this peak in the ground state entanglement corresponds to the bifurcation of the classical fixed point we are required to demonstrate some link between the parameter value at the bifurcation and the value for maximal entanglement. In the classical limit, the bifurcation occurs at $\mu_c = 1/L$. From the definition of the semi-classical variables Eq.(26), $L_{a\alpha} = \langle \hat{J}_{a\alpha} \rangle / \sqrt{j(j+1)}$, in the quantum regime, the *quantum* critical parameter, μ_{qc} , should follow

$$\mu_{qc} \propto \frac{1}{\sqrt{j(j+1)}}. \quad (38)$$

Guided by this expression and ignoring the spin- $\frac{1}{2}$ case, figure 7 is a plot of the inverse of the parameter value at the maximal entanglement, μ_{qc} against $\sqrt{j(j+1)}$, the total angular momentum of the individual subsystem corresponding to that μ_{qc} .

Clearly there is a linear relationship between $\frac{1}{\mu_{qc}}$ and j for all values except the spin- $\frac{1}{2}$ case. For large j , $\mu_{qc} = \frac{1}{j}$, so, in the classical limit

$$\mu_{qc} \rightarrow \mu_c \quad (39)$$

as predicted in conjecture 1.

To investigate the reasoning behind this prediction, we now consider the corresponding Husimi functions for the ground state.

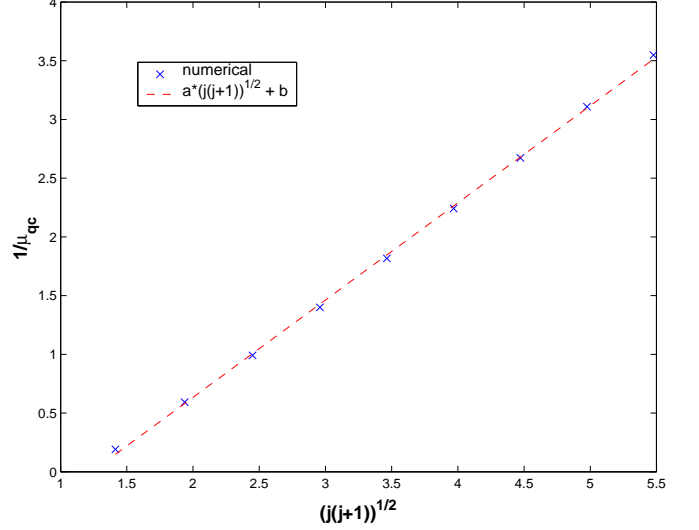


FIG. 7: The inverse of μ_{qc} , the value at which the entanglement in the ground state is maximum, against the total angular momentum of the individual subsystems j , with a line of best fit (ignoring the spin- $\frac{1}{2}$ case). The values of the parameters in the line of best fit are $a = 0.8385$ and $b = -0.6771$. See that as $j \rightarrow \infty$ and the system becomes more classical, the quantum critical parameter approaches the classical critical parameter i.e. $\mu_{qc} \rightarrow \mu_c$.

3. Phase-space distributions

In this section we consider the Q -function of the ground state with respect to varying values of the coupling μ . According to Sec. II C, the quantum ground state distribution should be localized on the coordinates of the stable classical fixed point, and as this point bifurcates, the distribution itself should bifurcate and spread to the two new stable fixed points, moving away from the (now) unstable fixed point.

Figure 8 shows the variation of the $\phi_1 = \phi_2 = \pi$ cross-section of the ground state Q -function as the coupling strength μ increases. Figure 9 is the entanglement in the ground state with respect to μ , with the value of the entanglement corresponding to each of the Q -functions in figure 8 so marked (all results are for $j = 5$).

Following this variation, it is clear that these numerical results concur with both theorem 1 and the reasoning behind the conjecture. For zero coupling, and hence zero entanglement, the Q -function is localized on the classical coordinates of the fixed point. This is also a coherent state, agreeing with the notion that separable states are coherent, and hence the most highly localized.

As the distribution varies with the increase in the coupling, it begins to stretch and spread out toward the two emerging stable fixed point coordinates at $(\theta_1, \theta_2) = (\pi, 0)$ and $(0, \pi)$, becoming less localized and hence increasingly more entangled. Corresponding to the maximal entanglement, the distribution is at its most delocal-

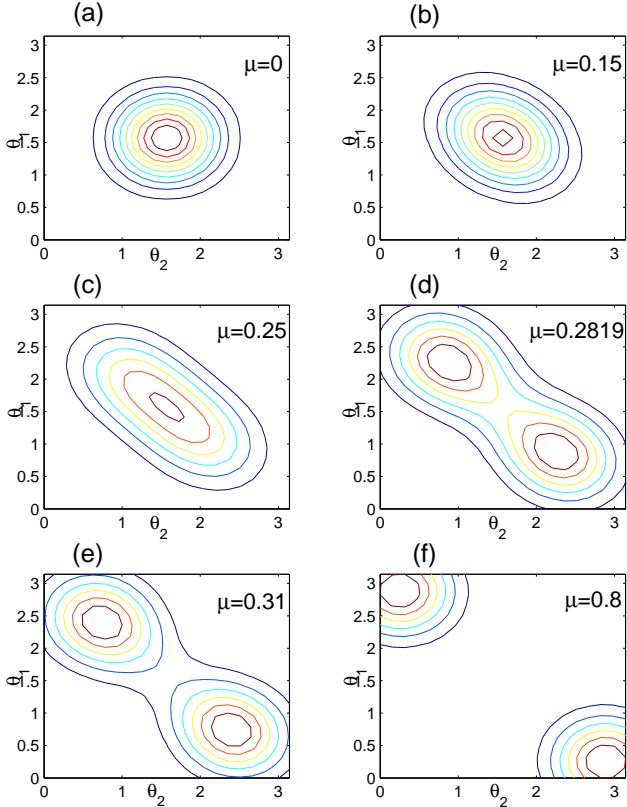


FIG. 8: The $\phi_1 = \phi_2 = \pi$ cross-sections of the ground state Q -function for a coupling strength μ of (a) 0, (b) 0.15, (c) 0.25, (d) 0.2819, (e) 0.31 and (f) 0.8. The entanglement corresponding to these states is shown in figure 9.

ized, spread between the two emergent fixed points. As the variation with respect to μ continues, the distribution begins to localize around the two fixed points and we approach the ‘twin-peaked’ *EPR*-state distribution.

As a counter-example, we now consider a system whose classical description exhibits a different type of bifurcation. The bimodal atom-molecule BEC is a much-studied model systems whose entanglement properties have only recently been studied.

IV. THE ATOM-MOLECULE BEC

The simplest, model two-mode atom-molecule BEC system comprises the coherent coupling between an atomic BEC and the corresponding (diatomic) molecular BEC, which constitute the two modes of the system. The simplest Hamiltonian which describes the two-mode atom-molecule BEC takes the form [34]

$$\hat{H}_{AM} = -\frac{\delta}{2}\hat{a}^\dagger\hat{a} - \frac{\Omega}{2}\left(\hat{a}^\dagger\hat{a}^\dagger\hat{b} + \hat{b}^\dagger\hat{a}\hat{a}\right) \quad (40)$$

where \hat{a}^\dagger and \hat{b}^\dagger denote the creation operators for the atomic and molecular modes, respectively, Ω is a mea-

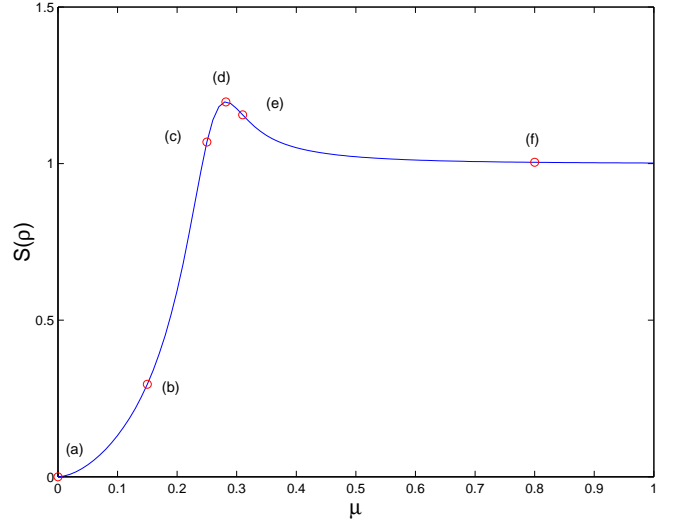


FIG. 9: The entanglement in the ground state, $S(\rho)$, with respect to coupling strength, μ , for $j = 5$. The circled points indicate the entanglement corresponding to the six Husimi distributions in Figure 8.

sure of the strength of the matrix elements for creation and destruction of molecules and δ is the molecular binding energy in the absence of coupling. The total atom number $\hat{N} = \hat{n}_a + 2\hat{n}_b$, where $\hat{n}_a = \hat{a}^\dagger\hat{a}$ and $\hat{n}_b = \hat{b}^\dagger\hat{b}$, commutes with the Hamiltonian, so is a constant of the motion.

We begin the analysis of the two-mode atom-molecule BEC with the semi-classical analysis which has been studied previously by Koštrum, Mackie, Côté and Javanainen [34]. In this case, we find the exact same stationary state solutions, but show that our stability analysis differs from that in Ref.[34].

A. Semi-classical Dynamics

Following Koštrum *et al.* [34], to derive an analytic solution for the semi-classical fixed points, we construct the *Kamiltonian*, K , by adding a scalar multiple of the conserved total particle number to the Hamiltonian,

$$\begin{aligned} K &= H + \gamma\hat{N} \\ &= -\frac{\delta}{2}\hat{n}_a + \frac{\Omega}{2}\left(\hat{a}^\dagger\hat{a}^\dagger\hat{b} - \hat{b}^\dagger\hat{a}\hat{a}\right) + \gamma(\hat{n}_a + 2\hat{n}_b) \quad (41) \end{aligned}$$

where γ is an arbitrary, real scalar, analogous to the chemical potential in thermodynamics. This addition has no effect on the dynamics, as it amounts to the addition of a constant energy term as the system must remain in an eigenstate of \hat{N} .

Now the semi-classical dynamics are analyzed, as before, by deriving the Heisenberg equations of motion for the annihilation and creation operators of the two modes, then taking the semi-classical limit, replacing the

operators with complex numbers. Letting $\hat{a} \rightarrow \sqrt{N}\Psi$, $\hat{b} \rightarrow \sqrt{N}\Phi$ so the corresponding creation operators are the complex conjugates, and defining the dimensionless parameter $\bar{\delta} = \delta/\Omega\sqrt{N}$, the semi-classical equations of motion become

$$\dot{\Psi} = -i(\bar{\delta} + \gamma)\Psi - 2i\Psi^*\Phi, \quad (42)$$

$$\dot{\Phi} = -2i\gamma\Phi - i\Psi^2, \quad (43)$$

and complex conjugates, with the constraint

$$|\Psi|^2 + 2|\Phi|^2 = 1 \quad (44)$$

which corresponds to the conservation of particle number.

Solving to find the fixed points yields the same solutions as found in [34]. The trivial solutions

$$\Psi_0^0 = \gamma_0^0 = 0, \Phi_0^0 = \pm\frac{1}{\sqrt{2}}, \quad (45)$$

for $\bar{\delta} \leq \sqrt{2}$,

$$\Psi_0^+ = \frac{\sqrt{6 - \bar{\delta}^2 - \bar{\delta}\sqrt{6 + \bar{\delta}^2}}}{3}, \quad (46a)$$

$$\Phi_0^+ = \frac{-\bar{\delta} - \sqrt{6 + \bar{\delta}^2}}{6}, \quad (46b)$$

$$\gamma^+ = -\Phi_0^+ \quad (46c)$$

and for $\bar{\delta} \geq -\sqrt{2}$,

$$\Psi_0^- = \frac{\sqrt{6 - \bar{\delta}^2 + \bar{\delta}\sqrt{6 + \bar{\delta}^2}}}{3}, \quad (47a)$$

$$\Phi_0^- = \frac{-\bar{\delta} + \sqrt{6 + \bar{\delta}^2}}{6}, \quad (47b)$$

$$\gamma^- = -\Phi_0^- \quad (47c)$$

Thus there are at least three stationary states for each $\bar{\delta}$, and four in the interval $-\sqrt{2} \leq \bar{\delta} \leq \sqrt{2}$. The stability analysis by Koštrum *et al* of these stationary states determined that any stationary state involving atoms is unstable. However, according to the stability criterion of Eq. (1), the purely molecular fixed point, $\Phi_0^0 = +1/\sqrt{2}$ becomes unstable for $\bar{\delta} > -\sqrt{2}$ and $\Phi_0^0 = -1/\sqrt{2}$ is unstable for all $\bar{\delta} < \sqrt{2}$. The other fixed points are always stable when defined. This allows us to create the bifurcation diagrams shown in figure 10.

The situation where one, stable fixed point loses its stability while another stable fixed point is formed, is known as a *transcritical* bifurcation [18]. We would not expect a peak in the entanglement of the stationary state to in any way correspond to this bifurcation, as we now demonstrate.

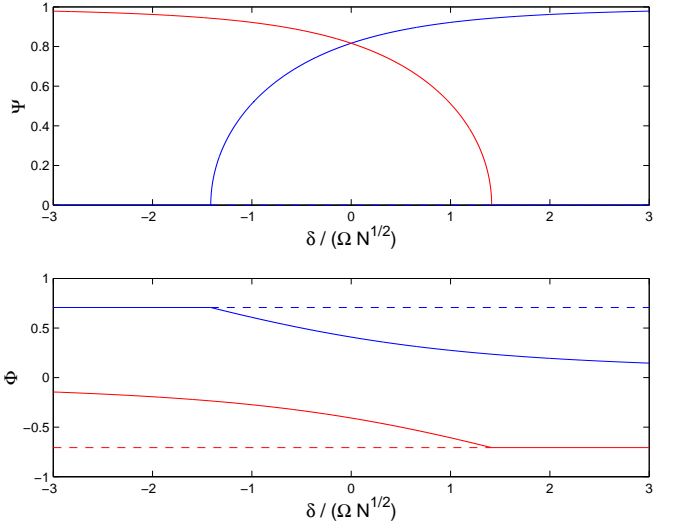


FIG. 10: Bifurcation diagrams for the stationary states of the atom-molecule BEC system. Again, a solid line indicates that the stationary state is stable, and a dashed line corresponds to instability. Clearly, there are two bifurcations, at $\delta/\Omega\sqrt{N} = \pm\sqrt{2}$, both of which are *transcritical*.

B. Entanglement Analysis

As argued previously [6], the only useful entanglements in two-mode BEC systems are those between the modes of the system as opposed to between the individual (indistinguishable) particles. A general state of the atom-molecule BEC system can be written in terms of the Fock basis states

$$|\chi\rangle = \sum_{n=0}^M d_n |2n\rangle |M-n\rangle \quad (48)$$

for where $M = N/2$, for an even atom number, N , while for odd N , the general state $|\phi\rangle$ can be expressed as

$$|\phi\rangle = \sum_{n=0}^M d_n |2n+1\rangle |M-n\rangle \quad (49)$$

where in this case, $M = (N-1)/2$ and the $\{d_n\}$ are complex coefficients.

The entropy of entanglement, $S(\rho)$, (where $\rho = |\chi\rangle\langle\chi|$), for these states is then given by [6]

$$S(\rho) = -\sum_{n=0}^M |d_n|^2 \log |d_n|^2. \quad (50)$$

To determine the stationary state corresponding to the classical bifurcating fixed points, we refer to Koštrum *et al.* [34] who identified the ground state of the atom-molecule BEC as corresponding to

$$\Phi_0 = \Phi_0^0, \Psi_0 = \Psi_0^0, \forall \bar{\delta} < -\sqrt{2} \quad (51)$$

$$\Phi_0 = \Phi_0^-, \Psi_0 = \Psi_0^-, \bar{\delta} \geq -\sqrt{2}. \quad (52)$$

This identification can be seen by comparing the average fraction of atoms in the ground state for the semi-classical solution with for the quantum-mechanical ground state, as shown in figure 11. The ground state of Hamiltonian (40) is found through direct numerical diagonalization.

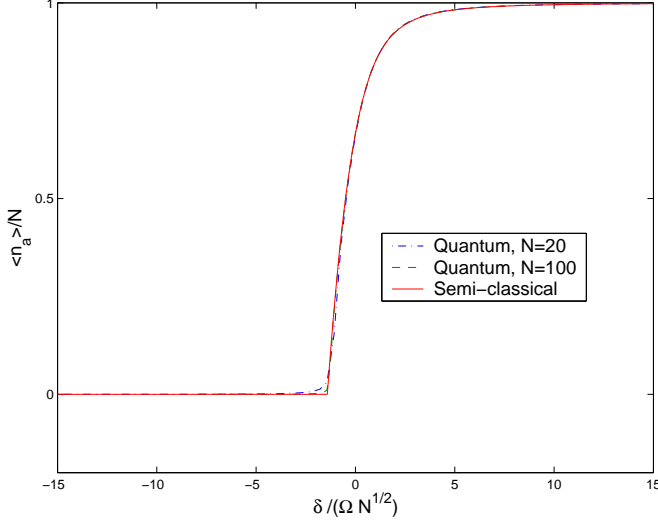


FIG. 11: The average fraction of atoms in the ground state for varying parameter δ . We see the excellent agreement between the quantum and semi-classical states even for small total atom number.

It is clear that there is excellent agreement between the semi-classical and quantum ground states. However, this identification of the ground state appears to contradict the stability analysis of Ref.[34] - the fixed point Φ_0^-, Ψ_0^- , according to their analysis, is unstable and so a stationary quantum distribution would not be localized around this region. This confirms the validity of our stability analysis and strengthens the agreement between the semi-classical and quantum stationary states.

Using Eq.(50), the entanglement in the ground state for varying parameter values δ and differing total particle number, N , were calculated and the results are shown in figure 12.

Clearly, the ground state entanglement does not exhibit a peak corresponding to the critical parameter value, $\delta = -\sqrt{2}$. This is expected, due to the nature of the bifurcation. In this case, the quantum distribution remains centred around the coordinates of one classical fixed point, and we would not expect it to exhibit the entanglement characteristics corresponding to a pitchfork bifurcation.

However, for Hamiltonian (40), in the limit of $N \rightarrow \infty$, there is a quantum phase transition in the ground state at $\bar{\delta} = -\sqrt{2}$ [35]. This is the threshold coupling for a predominantly molecular BEC. From figure 11, it is clear that at $\bar{\delta} = -\sqrt{2}$, the ground state changes from a totally molecular BEC ($\langle n_a \rangle = 0$), and that this change

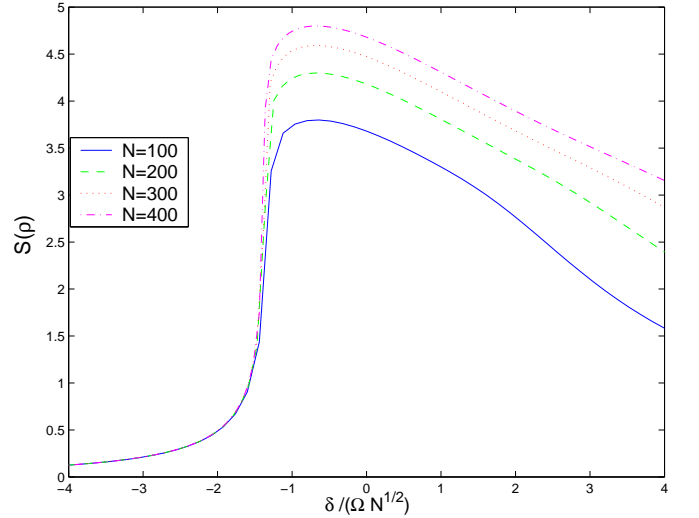


FIG. 12: The entropy of entanglement, $S(\rho)$, for the ground state of the atom-molecule BEC for different atom number N . Note that the maximum value of the entanglement does not occur at the value of $\delta/(\Omega\sqrt{N})$ at which the phase transition occurs (compare with figure 11).

is smooth in the quantum regime, but becomes non-analytic in the semi-classical solution. In the limit of infinite N , this is the quantum phase transition, where the ground state is no longer completely molecular, and the change in the atomic mode number is non-analytic. Thus, while the classical bifurcation in this case does not correspond to a peak in the ground state entanglement, it does correspond to the quantum phase transition in the two-mode atom-molecule BEC.

The two systems we have considered so far have had relatively simple fixed point structure, with only one type of bifurcation evident. We now move on to a more complicated example that exhibits a diverse fixed point structure.

V. COUPLED NONLINEAR TOPS

In Sec. III, we considered the simple model of two *linear* spinning tops coupled via a scalar interaction. A more realistic description [15] of the coupled magnetic clusters is as a system of *nonlinear* coupled tops, analogous to the models considered by Haake [36]. This nonlinearity to the individual spins comes in the guise of a \hat{J}_{zi}^2 term, describing the high anisotropy of the magnetic clusters [15].

$$\hat{H}_{nl} = \hat{J}_x + \alpha \hat{J}_z^2. \quad (53)$$

Retaining the nonlinear parameter, α , which we assume to be identical for the two tops, the entire compos-

ite system is described now by a two-parameter Hamiltonian,

$$\hat{H}_2 = \hat{J}_{x1} + \hat{J}_{x2} + \alpha (\hat{J}_{z1}^2 + \hat{J}_{z2}^2) + \mu \hat{J}_{z1} \hat{J}_{z2}. \quad (54)$$

Following the generic structure of this paper, we begin the analysis with the semi-classical dynamics.

A. Semi-classical Dynamics

The classical dynamics of the nonlinear coupled tops are described by the following equations of motion for the already defined semi-classical angular momentum variables $L_{\alpha i}$,

$$\dot{L}_{x1} = -\mu L_{y1} L_{z2} - 2\alpha L_{y1} L_{z1}, \quad (55a)$$

$$\dot{L}_{y1} = \mu L_{x1} L_{z2} - L_{z1} + 2\alpha L_{x1} L_{z1}, \quad (55b)$$

$$\dot{L}_{z1} = L_{y1}, \quad (55c)$$

$$\dot{L}_{x2} = -\mu L_{z1} L_{y2} - 2\alpha L_{y2} L_{z2}, \quad (55d)$$

$$\dot{L}_{y2} = \mu L_{z1} L_{x2} - L_{z2} + 2\alpha L_{x2} L_{z2}, \quad (55e)$$

$$\dot{L}_{z2} = L_{y2}, \quad (55f)$$

which correspond to the linear tops equations, with the additional terms coming from the nonlinearity.

The fixed point structure of the coupled nonlinear tops is much more complex than the corresponding linear tops model, as shown in figure 13 where $L = \alpha = 1$. The new parameter, α , in the Hamiltonian does not change the general classical fixed point structure.

Figure 13 indicates there are numerous bifurcations occurring as the coupling is increased from zero, much different from the coupled linear tops case. A full and detailed analysis of the nature of all fixed points and bifurcations occurring in this system is beyond the scope of this paper. Instead we focus on the two bifurcations that are pitchfork in nature, relating to the fixed points:

for $\alpha > 0$,

$$L_{x1} = L_{x2} = \pm L, \quad L_{z1} = L_{z2} = 0, \quad (56)$$

$$L_{x1} = L_{x2} = \frac{-1}{\mu - 2\alpha}, \quad L_{z1} = -L_{z2} = \pm f(\mu, \alpha) \quad (57)$$

and for $\alpha < 0$,

$$L_{x1} = L_{x2} = \pm L, \quad L_{z1} = L_{z2} = 0, \quad (58)$$

$$L_{x1} = L_{x2} = \frac{-1}{\mu - 2|\alpha|}, \quad L_{z1} = L_{z2} = \pm f(\mu, \alpha) \quad (59)$$

where

$$f(\mu) = \frac{((\mu - 2|\alpha| - \frac{1}{L}) (\mu - 2|\alpha| + \frac{1}{L}))^{1/2}}{\mu - 2|\alpha|}. \quad (60)$$

As with the linear tops case, $L_{y1} = L_{y2} = 0$ for all fixed points. Here we see that, since $\mu > 0$, the bifurcation's

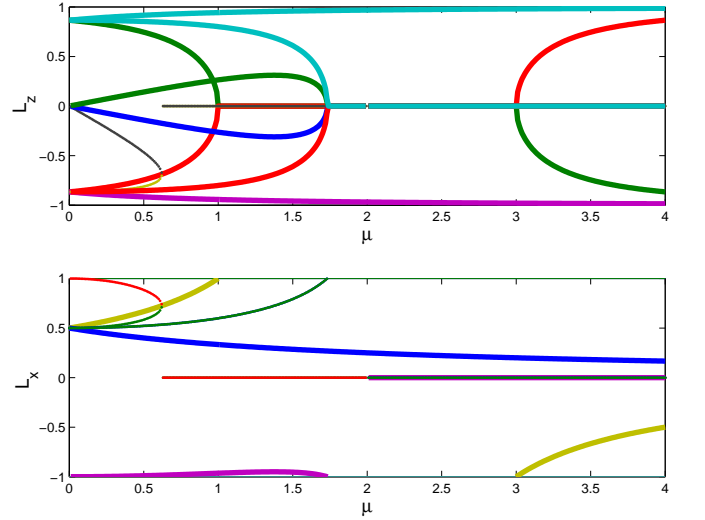


FIG. 13: The structure of the fixed points for varying coupling, μ , with $\alpha = 1$, for the coupled nonlinear tops system, with total subsystem angular momentum, $L = 1$. The above plots show the values of z - and x -components of the angular momentum of one of the tops (the plots are the same for either subsystem). The general fixed point structure is unaltered for varying α . Note that these fixed point plots do not show any information concerning the stability of the fixed points.

occur at the same values of μ for α positive or negative, so we restrict ourselves to $\alpha > 0$.

The fixed points in Eq.(56) exist for all values of μ . From Eq.(60), it is clear that the fixed points (57) do not exist in the parameter range $2\alpha - L^{-1} < \mu < 2\alpha + L^{-1}$. Corresponding to figure 13, the fixed point $L_{x1} = L_{x2} = -1$ bifurcates at $\mu = 3$ and the fixed point at $L_{x1} = L_{x2} = 1$ bifurcates at $\mu = 1$. This allows us to define the critical parameter value, μ_c as a function of the total angular momentum of each top,

$$\mu_c = 2\alpha \pm \frac{1}{L}. \quad (61)$$

Focusing on the bifurcation at $\mu_c = 2\alpha + \frac{1}{L}$, stability analysis shows that this is indeed a supercritical pitchfork bifurcation, with the originally stable $L_{x1} = L_{x2} = -1$ fixed point becoming unstable at the bifurcation, while the two emergent fixed points are stable. Compared to the expression for the critical coupling in the linear tops case Eq.(19), we see that the effect of the nonlinearity on the parameter value for the supercritical pitchfork bifurcation is to simply shift this critical parameter value in the positive μ direction, in proportion to the strength of the nonlinearity, α . So while the global fixed point structure for the coupled nonlinear tops system is substantially more complex than the linear case, there does exist a supercritical pitchfork bifurcation which again corresponds to a peak in the quantum ground state entanglement.

B. Entanglement Analysis

As with the linear tops model, the fixed point exhibiting the supercritical bifurcation corresponds to the ground state of the coupled nonlinear tops systems - for $\mu = 0$, ground state is $|-j, -j\rangle_x$. Note that for $\alpha < 0$, the state undergoing the pitchfork bifurcation corresponds not to the ground state, but the highest excited stationary state (see Appendix A). Following the same approach as in Sec.III, the entanglement in the ground state of the coupled nonlinear tops system was found by direct numerical diagonalization of Hamiltonian (54), in the tensor product basis of the irreducible representations of $SU(2)$. Figure 14 displays the results for the entanglement in the ground state for $\alpha = 1$ (the value of α has no effect on the general characteristics of the entanglement).

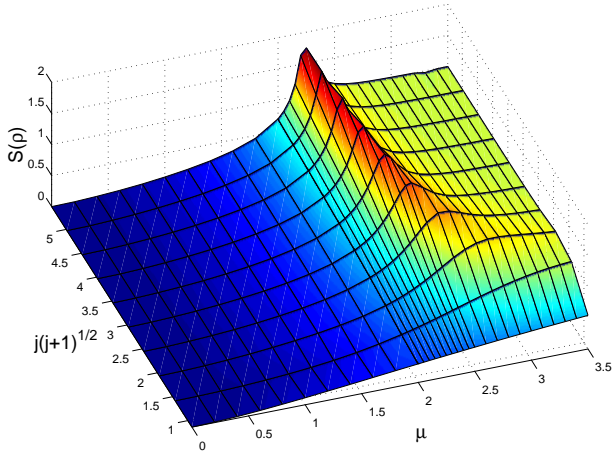


FIG. 14: The entanglement in the ground state of the system of coupled nonlinear tops for vary coupling, μ and subsystem angular momentum, j , with $\alpha = 1$. Note that as the system becomes more classical as j increases that the peak in the entanglement versus μ becomes more evident.

We note now that in the spin- $\frac{1}{2}$ case, there is no nonlinearity since the Pauli spin operators square to give the identity. Hence the $j = \frac{1}{2}$ results here are the same as those of the linear tops case, in Subsec III B. For $j > \frac{1}{2}$, the entanglement characteristics are similar to the linear tops case, with a peak in the entanglement at a finite μ . This characteristic peak becomes more pronounced as j increases. For $\mu \rightarrow \infty$, the Hamiltonian is the same in both the linear and nonlinear tops case, so the entanglement in the ground state asymptotes to 1.

Analogous to Sec.III, the value of μ at which the ground state entanglement was maximum (denoted μ_{qc}) was determined for increasing values of j . Guided by the relation between the classical critical parameter value (μ_c) and total subsystem angular momentum (L), figure 15 shows plot of j against $(\mu_{qc} - 2)^{-1}$.

The linear relationship between $\sqrt{j(j+1)}$ and $(\mu_{qc} - 2)^{-1}$ again illustrates that the peak in the entangle-

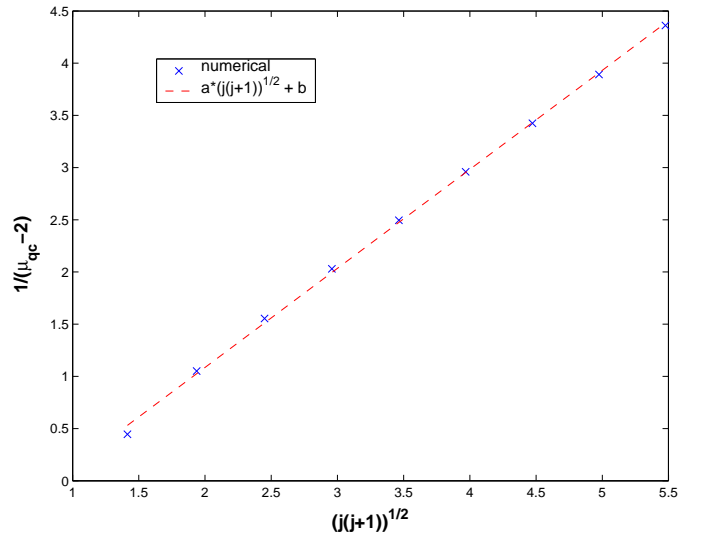


FIG. 15: The relationship between the quantum critical parameter values, μ_{qc} and the total angular momentum of the individual subsystems. The parameters in the line of best fit are $a = 0.9618$ and $b = -0.4172$. See that as $j \rightarrow \infty$ and the system becomes more classical, the quantum critical parameter approaches the classical critical parameter i.e. $\mu_{qc} \rightarrow \mu_c$

ment corresponds to the bifurcation of the classical fixed points, i.e. in the classical limit

$$\mu_{qc} \rightarrow \mu_c. \quad (62)$$

. In this case, even though other bifurcations exist, the supercritical pitchfork bifurcation still corresponds to a peak in the corresponding quantum ground state entanglement.

VI. CONCLUSION

We have demonstrated that there is a direct relationship between entanglement and a certain type of classical bifurcation. At a supercritical pitchfork bifurcation in the classical regime of a multipartite systems, the entanglement in the quantum ground state, as a function of the bifurcation parameter, is a maximum. This is another example of where the maximal entanglement does not correspond to the strongest interaction but rather to some critical phenomena. In this case, that critical phenomena is classical, as opposed to the relationships between quantum phase transitions entanglement, as demonstrated by Osborne and Nielsen [1] and Osterloh, Amico, Falci and Fazio [2] among others.

The understanding of entanglement is at the very heart of quantum information theory. The study of the entanglement characteristics of simple many-body systems provides a basis for further studies into more complex, and realistic systems with the hope of one day applying the results to 'real-world' quantum computing.

Acknowledgments

The authors would like to thank Benjamin Skellett and Tobias Osborne for valuable discussions and Michael

Bremner and Mohan Sarovar for assistance with the manuscript. APH especially thanks Benjamin Skellett for assistance the figures in section III A. This work has been supported by the Australian Research Council.

[1] T. Osborne and M. Nielsen, Phys. Rev. A **66**, 032110 (2002).

[2] A. Osterloh, L. Amico, G. Falci and R. Fazio, Nature **416**, 608 (2002).

[3] G. Vidal, J.I. Latorre, E. Rico and A. Kitaev, Phys. Rev. Lett **90**, 227902 (2003).

[4] J.I. Latorre, E. Rico and G. Vidal, quant-ph/0304098.

[5] T. Costi and R.H. McKenzie, to appear in Phys. Rev. A, quant-ph/0302055.

[6] A.P. Hines, R.H. McKenzie and G.J. Milburn, Phys. Rev. A **67**, 013609 (2003).

[7] U. Dorner, P. Fedichev, D. Jaksch, M. Lewenstein and P. Zoller, quant-ph/0212039.

[8] G.J. Milburn, R. Laflamme, B.C. Sanders and E. Knill, Phys. Rev. A **65**, 032316 (2002).

[9] J. Emerson and L.E. Ballentine, Phys. Rev. A **63**, 052103 (2001).

[10] J.V. Emerson, Ph.D. thesis, Simon Fraser University (2001).

[11] G.P. Berman, G.D. Doolen, G.V. Lopez and V.I. Tsifrinovich, quant-ph/9802015.

[12] B.E. Kane, Nature **393**, 133 (1998).

[13] H. Fujisaki, T. Miyadera and A. Tanaka, quant-ph/0211110.

[14] S.Schneider and G.J.Milburn, Phys. Rev. A **65**, 042107 (2002).

[15] J. Tejada, E.M Chudnovsky, E. del Barco, J.M. Hernandez and T.P. Spiller, Tech. Rep. HPL-2000-87, Hewlett Packard Laboratories (2000).

[16] B.Skellett and C.A.Holmes, Interjournal Complex Systems **51** (2002), www.interjournal.org.

[17] A.P. Hines and G.J. Milburn, unpublished.

[18] P. Glendinning, *Stability, instability and chaos: an introduction to the theory of nonlinear differential equations* (Cambridge University Press, 1994).

[19] J. Preskill, <http://www.theory.caltech.edu/people/preskill/ph229/#lecture> (Chap. 5).

[20] M.A. Nielsen and I.L. Chuang, *Quantum computation and quantum information* (Cambridge University Press, Cambridge, 2000).

[21] M. Latka, P. Grigolini and B.J. West, Phys. Rev. A **47**, 6 (1993).

[22] G.J. Milburn, Phys. Rev. A **33**, 1 (1986).

[23] E.P. Wigner, Phys. Rev. **40**, 749 (1982).

[24] B.C. Sanders, Phys. Rev. A **40**, 5 (1989).

[25] W.A. Lin and L.E. Ballentine, Phys. Rev. Lett. **65**, 24 (1990).

[26] S.B. Lee and M.D. Feit, Phys. Rev. E **47**, 6 (1993).

[27] D. Appleby, Int. J. Theor. Phys. **39**, 2231 (2000).

[28] A. Perelomov, *Generalized Coherent States and Their Applications* (Springer-Verlag, Berlin, 1986).

[29] A. Sugita, nlin/0112042.

[30] R. Gilmore, Ann. Phys., NY **74**, 391 (1972).

[31] D.Gunlycke, S.Bose, V.M.Kendon and V.Vedral, Phys. Rev. A **64**, 042302 (2001).

[32] W.K. Wootters, Phys. Rev. Lett. **80**, 2245 (1998).

[33] S. Sachdev, *Quantum phase transitions* (Cambridge University Press, Cambridge, 1999).

[34] M. Koštrum, M. Mackie, R. Côté and J. Javanainen, Phys. Rev. A **62**, 063616 (2000).

[35] H.-Q. Zhou and J. Links and R.H. McKenzie, cond-mat/0207540.

[36] F. Haake, *Quantum Signatures of Chaos* (Springer, Berlin, 1991).

[37] The definition of stability used here refers to asymptotic stability. There are, in fact many differently defined notions of stability.

[38] Note the factor of 2 that does not appear in this expression in [31] - this must be a typographical error.